Journal of Thermal Analysis, Vol. 42 (1994) 1251-1263

THERMOANALYTICAL INVESTIGATIONS OF DECOMPOSITION COURSE OF COPPER OXYSALTS I. Basic copper carbonate

S. A. A. Mansour

Chemistry Department, Faculty of Science, Minia University, El-Minia, Egypt

(Received May 4, 1993)

Abstract

The thermal decomposition of basic copper carbonate (malachite; $CuCO_3 \cdot Cu(OH)_2$) in a dynamic atmosphere of air or nitrogen was studied via TG, DTA and DSC at different heating rates. The non-isothermal kinetic and thermodynamic parameters were estimated. The decomposition course was thoroughly followed by examining the structural and morphological consequences of calcining the material at elevated temperatures by IR, XRD and SEM. The results obtained showed that in air $CuCO_3 \cdot Cu(OH)_2$ released 0.5 H_2O at 195°C, transforming into the azurite structure $2CuCO_3 \cdot Cu(OH)_2$. Decomposition then commenced, through two endothermic steps maximized at 325 and 430°C. The resultant product maintained the water released from the decomposition process up to 650–750°C. A schematic decomposition pathway has been proposed in terms of the thermal and physicoanalytical results.

Keywords: basic carbonates, copper carbonates, kinetics, thermodynamic parameters

Introduction

Basic carbonates are appropriate initial compounds for the preparation of highly dispersed metal oxides, and therefore their thermal decomposition has acquired profound importance. These carbonates were classified [1] into three categories on the basis of the thermal decomposition mechanism, i.e. H_2O and CO_2 are evolved: (i) at the same temperature, (ii) in subsequent steps or (iii) in different steps, H_2O being evolved first.

Basic copper carbonate, the target of the present investigation, was reported [1] to lie in class (i). It occurs in nature as azurite, $2CuCO_3 \cdot Cu(OH)_2$, or malachite, $CuCO_3 \cdot Cu(OH)_2$. The thermal decompositions of these compounds have been the subject of several investigations. Ramamurthy *et al.* [2] reported that the kinetics of thermal decomposition of basic copper carbonate is described by the Prout-Tompkin equation, while Zivkovic *et al.* [3, 4] applied a semidirect method in a static air atmosphere and concluded that the decomposition of basic

0368–4466/94/ $ 4.00

John Wiley & Sons, Limited
Chichester

copper carbonate follows first-order kinetics and that ΔE and ΔH are equivalent. Furthermore, Dollimore *et al.* [5, 6] studied the decomposition of basic copper carbonate both isothermally and non-isothermally in nitrogen and also concluded that the decomposition mechanism follows first-order kinetics, and described the compensation by the equation $\ln A = aE + b$. On the other hand, Uzunov and Klissurski [7] proposed that the mechanism of the decomposition of basic copper carbonate involves either two-dimensional or three-dimensional growth of nuclei, with a constant nucleation rate, leading to a linearly increasing number of nuclei, which is controlled by the chemical reaction proceeding on the surface of the new solid phase being formed. Recently, Henmi *et al.* [8, 9] demonstrated that the temperature of decomposition of basic copper carbonate was strongly influenced by the partial pressure of carbon dioxide.

The effect of the self-generated gases on the thermal decomposition of basic copper carbonate is evinced from the above-mentioned studies. To avoid such effect, the present work was conducted in a dynamic atmosphere of air or nitrogen, at different heating rates, in an attempt to reach a better understanding of the often conflicting reports already published. The decomposition course was followed by characterizing the decomposition product and the intermediate(s), a number of physical tools being adopted.

Experimental

Materials

Reagent grade (99.9% pure) basic copper carbonate, (Chemische Fabrik Erich Nickel-Schmalkalden (Tür), Germany), was the material used for this study. It will be denoted in the text as BCuC. From thermal analysis (see below), solid-phase decomposition products were obtained by heating at 250–1050°C for 2 h in still air, and then kept dry over $CaCl_2$ for further investigations.

Thermal analysis

Thermogravimetry (TG), differential thermal analysis (DTA) and differential scanning calorimetry (DSC) of BCuC were performed with an automatically recording Shimadzu 30H analyser (Japan), on heating up to 1050°C at various rates (θ = 5, 10, 20 and 50 deg·min^{-1}) in a dynamic (30 ml·min^{-1}) atmosphere of air for TG and DTA and of nitrogen for DSC. The heat of transition (28.24 J·g^{-1} [10]) of specpure indium metal (Johnson-Matthey) at 157°C was adopted for the DSC calibration. Non-isothermal kinetic parameters (k, A, and ΔE) were determined from the effects of the heating rate on the temperatures (T_{max}) at which the mass-variant (TG), invariant (DTA) and DSC peaks of the

thermal events encountered are maximized, adopting Ozawa methods [11, 12]. DSC data were further used to calculate the thermodynamic parameters (ΔH, C_p and ΔS) [13, 14]. The mathematical procedures were described in detail earlier [15].

Infrared spectroscopy (IR)

IR spectra of BCuC and its solid calcination products were obtained at a resolution of 5.3 cm^{-1}, over the frequency range 4000–250 cm^{-1}, using a Perkin-Elmer 580B double-beam spectrophotometer (UK), with the KBr technique.

X-ray diffractometry (XRD)

X-ray powder diffractograms of BCuC and its calcination products were obtained with a JSX-60 PA Jeol diffractometer (Japan), using Ni-filtered CuK_α radiation. The diffraction pattern ((I/I°) *vs.* d-spacing (Å)) thus obtained was matched with the relevant ASTM standards [16].

Electron microscopy (SEM)

Samples of BCuC and its calcination products were examined in a Jeol 35CF scanning electron microscope. The samples were mounted for viewing and coated with a thin layer of gold to render them conducting. The photographs presented here illustrate typical and reproducible structures that are considered to be significant.

Results and discussion

Figure 1 shows TG and DTA curves of the thermal decomposition of BCuC in a dynamic atmosphere (30 $ml \cdot min^{-1}$) of air at heating rates θ = 5, 10, 20 and 50 $deg \cdot min^{-1}$. The Figure indicates that the material loses $\approx 24\%$ of its original mass on heating up to 500°C, through three successive endothermic events, maximized at 195°C (I), 325°C (II) and 430°C (III), respectively. The TG curves show a further mass loss event (IV) in the temperature range 650–750°C, detected only in the DTA curve obtained at a heating rate of 50 $deg \cdot min^{-1}$ (the highest heating rate used). Figure also indicates the effects of variation of the heating rate on the T_m of the encountered events. For convenience, the characterization of these events will be discussed in terms of the TG and DTA curves recorded at θ = 10 $deg \cdot min^{-1}$.

The IR spectra and XRD powder diffractograms of BCuC and its calcination products were used to characterize the encountered events.

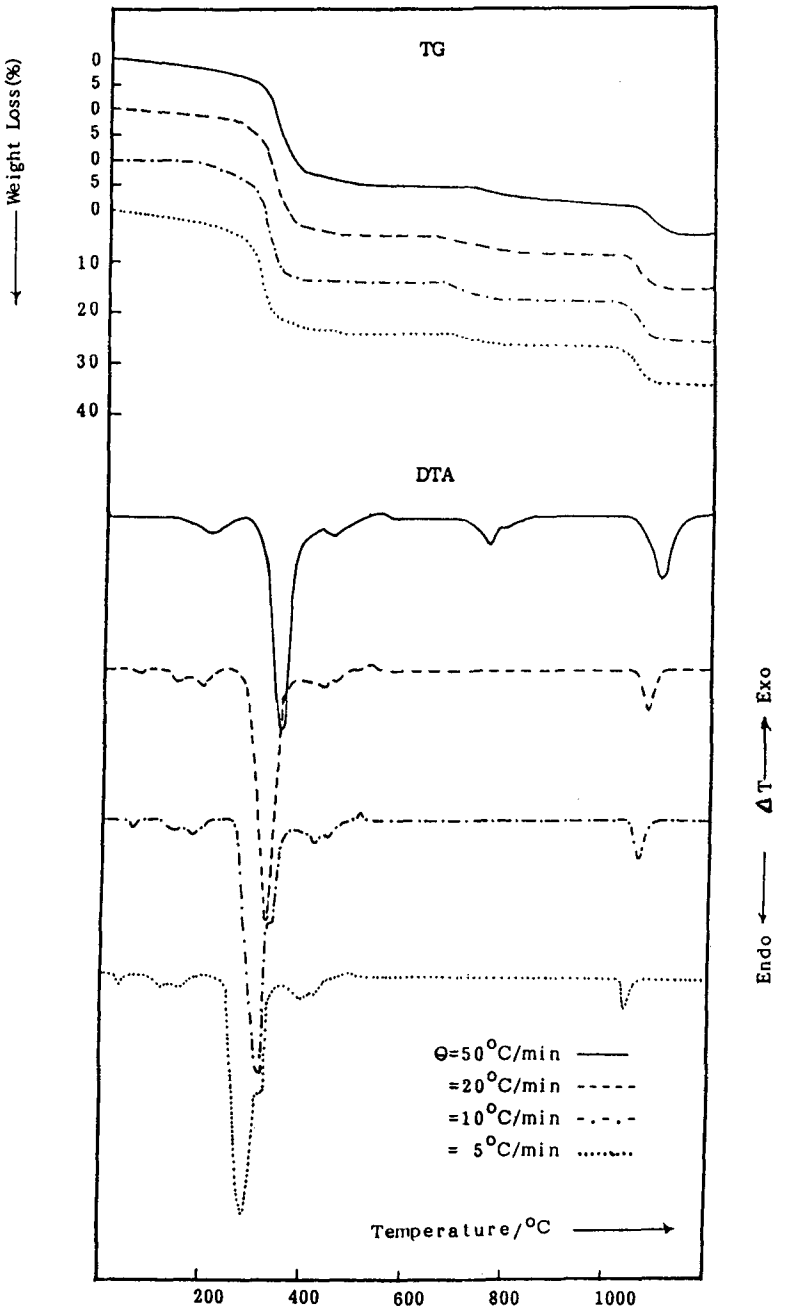

Fig. 1 TG and DTA curves of BCuC at the heating rates (θ) indicated, in a dynamic atmosphere (30 ml·min^{-1}) of air

The IR spectrum of the parent material exhibited all the absorption bands characteristic of $CuCO_3 \cdot Cu(OH)_2$ [2, 17]. Furthermore, its XRD pattern displayed the characteristic lines of $CuCO_3 \cdot Cu(OH)_2$ [ASTM Card no. 10-399]. These results indicate that the parent material had the malachite structure of basic copper carbonate.

Figure 2 shows the TG and DTA curves of BCuC in a dynamic (30 $ml \cdot min^{-1}$) nitrogen atmosphere.

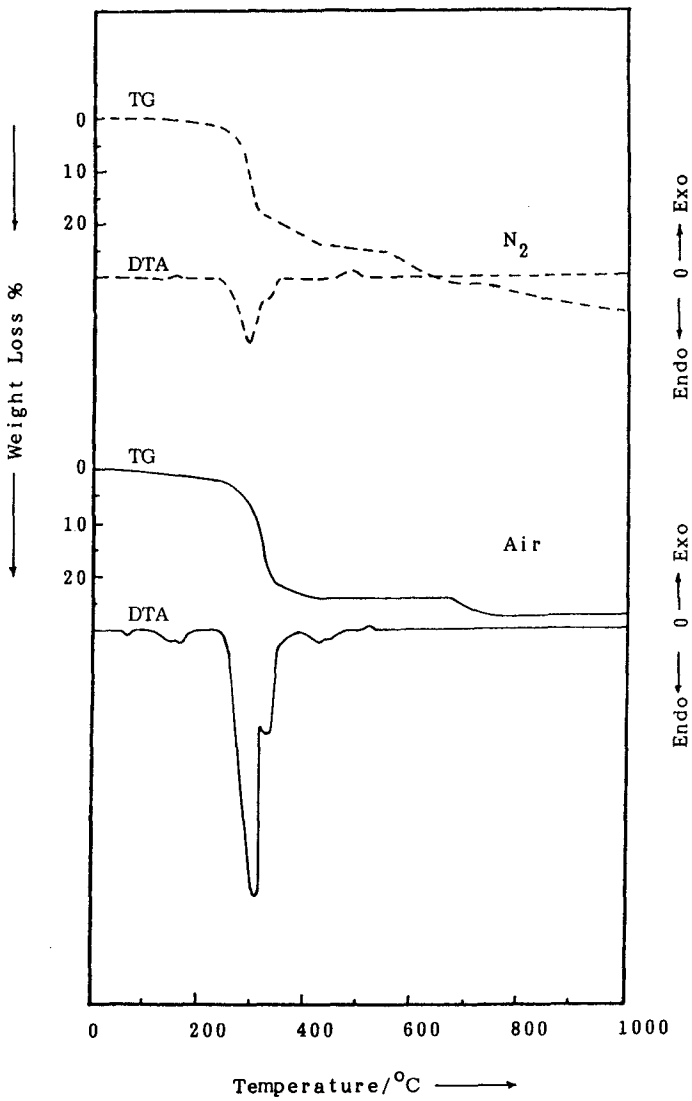

Fig. 2 TG and DTA curves of BCuC at 10 $deg \cdot min^{-1}$ in a dynamic atmosphere (30 $ml \cdot min^{-1}$) of nitrogen (– – –) or air (——)

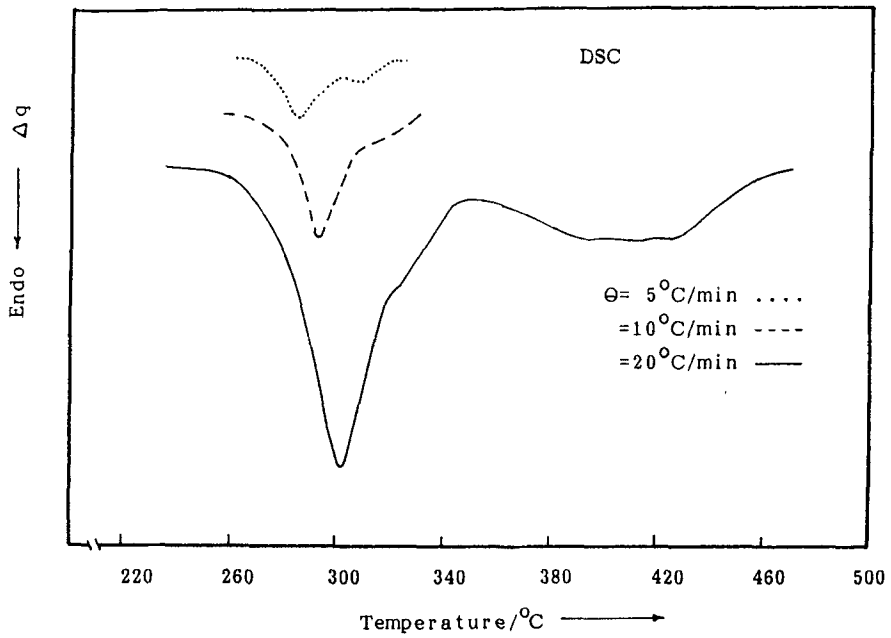

Fig. 3 DSC curves recorded for BCuC at the heating rates (θ) indicated, in dynamic atmosphere (30 ml·min^{-1}) of nitrogen

DSC curves recorded at heating rates of 5, 10 and 20 deg·min^{-1} are given in Fig. 3. The Figure clearly indicates that the last thermal process was detected only in the experiment carried out at the highest heating rate used (i.e. 20 deg·min^{-1}). log θ *vs.* $1/T_m$ plots were constructed for the encountered thermal events on the basis of the TG or DSC results and then used to calculate ΔE values. Non-isothermal kinetic parameters obtained from the TG and DTA results are given in Table 1, while Table 2 lists the non-isothermal kinetic and thermodynamic parameters derived from the DSC results.

Characterization of the encountered thermal events

Event I

Event I is shown by the DTA curves (Fig. 1) to be endothermic in nature. This event is maximized at 95°C and terminated at 250°C, with a 4% loss of the original mass. The IR spectrum of the decomposition product at 250°C displayed the absorption bands of the carbonate ion, and also the absorption band of νO–H at 3425 cm^{-1} [17], but with much lower intensity than that of the parent material, in addition to the disappearance of the doublet feature of its peak

shape. Such an appearance of one band for νO–H instead of the initial doublet is assigned to the azurite structure $2CuCO_3 \cdot Cu(OH)_2$ [17], the remainder of its absorption bands also being displayed in the spectrum. The XRD of the decomposition product at 250°C indicated that the material has lost its crystallinity through event I, giving rise to an amorphous product.

Table 1 Non-isothermal kinetic parameters of the thermal events encountered throughout the decomposition course of BCuC in air atmosphere (from TG results)

Thermal event	ΔE / kJ·mol^{-1}	k / min^{-1}	log A
I	156	$6.6 \cdot 10^{-2}$	13.8
II	200	$3.2 \cdot 10^{-2}$	16.4
III	230	$2.5 \cdot 10^{-3}$	18.6
IV	303	$2.1 \cdot 10^{-3}$	19.2

Table 2 Non-isothermal kinetic and thermodynamic parameters of the DSC responded events encountered throughout the decomposition of BCuC in nitrogen atmosphere

Thermal event	ΔE / kJ·mol^{-1}	ln A	k / min^{-1}	ΔH / kJ·mol^{-1}	C_p / J·g^{-1}·K^{-1}	ΔS / J·g^{-1}·K^{-1}
I	174	36.6	$65 \cdot 10^{-2}$	22.9	1.86	0.20
II	227	46.6	$80 \cdot 10^{-2}$	5.1	0.76	0.06

The loss in mass corresponding to this event (4%) is almost equal to the value calculated for the loss of half a mole of water per mole of BCuC. From these results, it could be concluded that the heating of BCuC up to 250°C in dynamic air resulted in transformation of the parent carbonate from the malachite ($CuCO_3 \cdot Cu(OH)_2$) into the azurite structure ($2CuCO_3 \cdot Cu(OH)_2$). In an earlier study [18], a decomposition step was observed for BCuC at about 95°C, which could obviously be attributed to such a transformation. The non-isothermal activation energy (ΔE) for this event (Table 1) amounts to 165 kJ·mol^{-1}, which could account for the destruction of the molecular arrangement.

Events II and III

Events II and III are shown by the DTA curves (Fig. 1) to be overlapping endothermic processes maximized at 310 and 450°C, respectively (curve recorded at 10 deg·min^{-1}). The corresponding TG curve shows that these two events bring the total loss up to 24% of the original mass. The IR spectrum of the decomposition product at 380°C displayed rather low intensities of the carbonate absorp-

tions, in addition to those assigned to the OH absorptions at 3425 and 1640 cm^{-1} [17]. Moreover, the IR spectrum of the decomposition product at 550°C displayed only the absorptions of OH in addition to ill-resolved absorption bands due to CuO [19]. On the other hand, the XRD of the calcination product at 380°C showed the pattern of CuO [ASTM Card no. 5–661]. The characteristic CuO lines were more pronounced in the XRD of the decomposition product at 550°C.

Since the first dehydration step (in event I) is the transformation of malachite into azurite, events II and III most probably involve the decomposition of azurite. The total mass loss by the end of event III (i.e. 24%), together with the appearance of the IR absorption bands of water in the calcination product at 550°C, support the formation of $CuO{\cdot}H_2O$ in this decomposition product. The commencement of the decomposition through the two overlapping events II and III (Fig. 1) would confirm that the decarbonation and dehydroxylation processes occurred separately.

Event IV

Figure 1 shows that event IV commenced endothermically (DTA at 50 $deg{\cdot}min^{-1}$) in the temperature range 650–750°C, with a 4% loss of the original mass. The IR spectrum of the decomposition product at 900°C revealed the complete removal of water. Weak absorptions in the range 700–350 cm^{-1} were observed, which are due to CuO [19]. The XRD of this decomposition product displayed the documented characteristic lines of CuO [ASTM Card no. 5-661], with very low-intensity lines of Cu_2O [ASTM Card no. 5-667]. From these results and the corresponding mass loss (4%), it is very likely that process IV involves the release of the retained H_2O. The high activation energy (ΔE) for this event (Table 2) may suggest that this process is largely deceleratory.

In conclusion, the course of thermal decomposition of basic copper carbonate, malachite ($CuCO_3{\cdot}Cu(OH)_2$), in dynamic air may include the following pathway:

$$2[CuCO_3{\cdot}Cu(OH)_2] \xrightarrow[-H_2O]{I} 2CuCO_3{\cdot}Cu(OH)_2 + CuO$$

$$2CuCO_3{\cdot}Cu(OH)_2 + CuO \xrightarrow{II} 3CuO + Cu{\cdot}H_2O + 2CO_2\uparrow + H_2O\uparrow$$

$$3CuO + Cu{\cdot}H_2O \xleftarrow{III} 3CuO + Cu(OH)_2 + 2CO_2\uparrow$$

$$4CuO + H_2O\uparrow \xrightarrow{>850°C} (4-x)CuO + xCu_2O$$

Figure 2 reveals that the thermal decomposition of BCuC under a nitrogen atmosphere commences at lower temperature than in air. The DTA curve in a nitrogen flow shows an endothermic peak maximized at 295°C with a shoulder at 325°C, corresponding to mass loss processes. The total mass loss accompanying these processes is almost equal to that in air. Therefore, the final decomposition product ought to be the same (i.e. CuO).

The decomposition of BCuC under a nitrogen flow has been reported [6] to follow either of the following two postulated schemes:

$$1.\ CuCO_3 \cdot Cu(OH)_2 \rightarrow 2CuO + CO_2 + H_2O \quad (A)$$

$$2.\ CuCO_3 \cdot Cu(OH)_2 \rightarrow CuCO_3 + CuO + H_2O$$

$$CuCO_3 \rightarrow Cu_2OCO_3 + CO \quad (B)$$

$$Cu_2OCO_3 \rightarrow 2CuO + CO_2$$

The TG curve obtained in a nitrogen flow (Fig. 4a) shows three rates of mass loss corresponding to the DTA endothermic processes. Hence, it appears most logical to presume that the decomposition of BCuC in dynamic nitrogen commenced through the postulated [6] scheme (B).

It is noticeable from Figs 1 and 2 that the obtained CuO dissociated at a higher temperature (≥ 850°C) in an air flow than in nitrogen, where this process took place at ~750°C.

DSC analysis (Fig. 3) demonstrates two overlapping endothermic processes in the temperature range 255–330°C (curve recorded at 10 deg·min^{-1} heating rate). The activation energies (ΔE) calculated from the DSC results for these two processes are 194 and 227 kJ·mol^{-1} (Table 2). These values are very close to those obtained from the TG results in an air flow (Table 1) for events II and III. It is to be noted that the enthalpy change (ΔH) corresponding to event I escaped detection on DSC analysis even at the highest heating rate applied (20 deg·min^{-1}), suggesting that the decomposition of the BCuC used (malachite) in nitrogen did not involve event I which occurred in air.

Electron microscopic studies

Attempts were made to correlate the structural and morphological changes accompanying the decomposition of BCuC with the corresponding physicochemical measurements. The SEM specimens were prepared from the same batches of material used in the XRD and IR analyses.

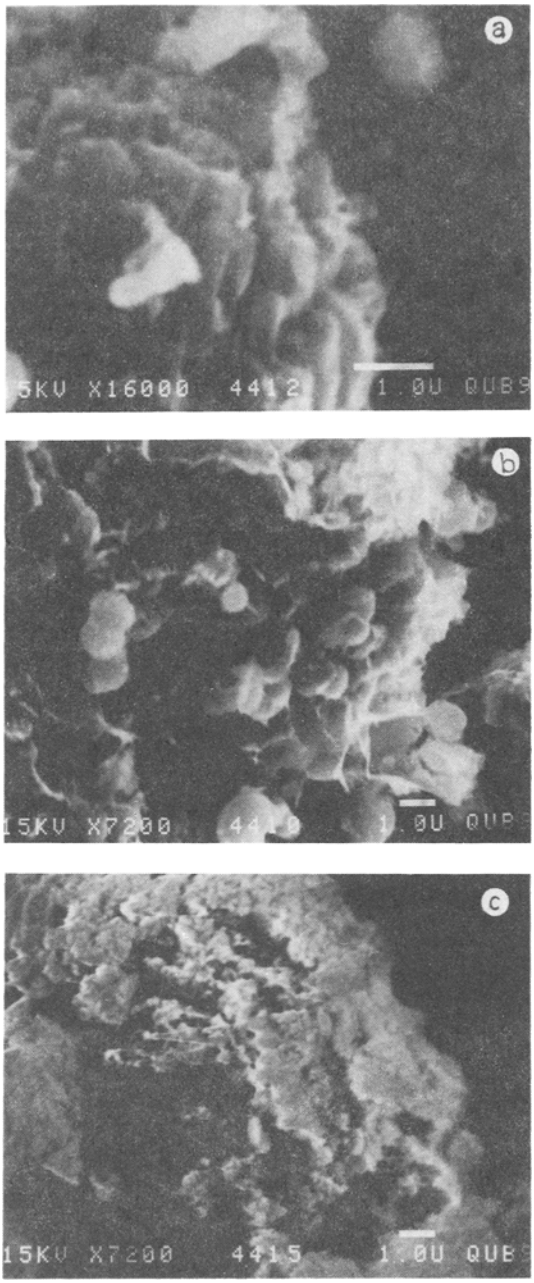

Fig. 4 Scanning electron micrographs of the calcination product of BCuC at 250°C, showing a grain surface (*a*); the product was composed of irregular particles (*b*); calcined at 350°C, revealing new surface features growing inwards (*c*)

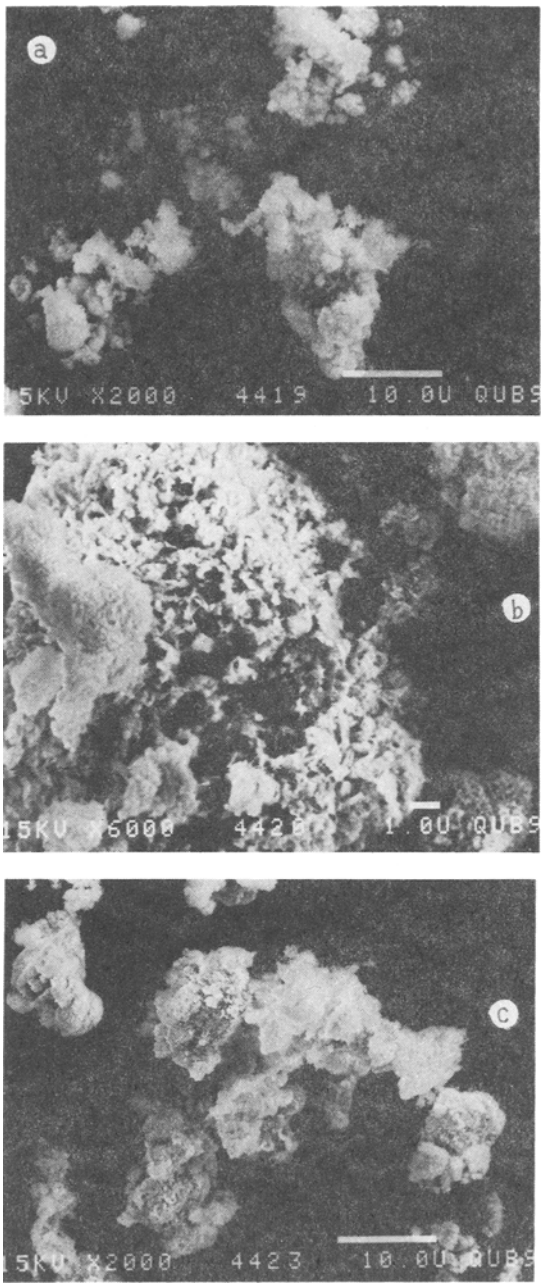

Fig. 5 Scanning electron micrographs of BCuC calcined at 380°C, showing a typical grain surface and aggregates of compact grains (*a*); calcined at 550°C, revealing a new crystallite assemblage (*b*), aggregated in coherent grains (*c*)

SEM studies of the parent BCuC revealed that the material was composed of grains of aggregate spheres of almost the same size. Electron micrographs could not be taken of the parent BCuC because it suffered strong charging by the electron beam.

Samples that had been calcined at 250°C showed marked changes in the morphology of the material, the most significant feature observed being the change in the spherical shape of the small particles and hence a marked change in the grain surfaces (Fig. 4a). The new structure was obviously not crystalline and was composed of irregular particles, as shown in Fig. 4b. These observations are in accordance with the thermal, IR and XRD analysis results, where event I involved the transformation of crystalline malachite into amorphous azurite.

The decomposition product at 350°C displayed marked phenomenological changes, where a new structure seemed to initiate on the surface and grow inwards, as seen in Fig. 4c, for a partly fractured grain. Such phenomenological features appeared clearly for samples calcined at 380°C, where the structure cohered and covered a great portion of the grain surfaces. Such coherence extended, giving rise to a micrograph of slightly compact grains (Fig. 5a). These results are in accordance with the thermal and XRD analyses, which indicated the formation of a crystalline decomposition product in this stage.

At 550°C, the development of the new crystallites was most noticeable (Fig. 5b). The structural coherency of the crystallites was still observed (Fig. 5c). Two crystallites appeared in this calcination product, as is clear from Fig. 5b. This in turn is also in good agreement with the thermal and IR analyses, which indicated that complete transformation into CuO occurred in a higher temperature range (650–750°C). The calcination product at 900°C was severely damaged by the electron beam and could not be photographed.

* * *

It is a pleasure to thank the Queen's University of Belfast, and particularly the staff of the Electron Microscope Unit, for assistance in obtaining the electron micrographs. Thanks also are due to the Egyptian Government for the granted Fellowships.

References

1 M. Kato and N. Mizutani, Koubutu Gaku Zasshi, 14 (1980) 15.
2 P. Ramamurthy and E. A. Secco, Canadian J. Chem., 48 (1970) 3510.
3 Z. D. Zivkovic, D. F. Bogosavljevic and Zlatkovic, Thermochim. Acta, 18 (1977) 235.
4 Z. D. Zivkovic, D. F. Bogosavljevic and Zlatkovic, Thermochim. Acta, 18 (1977) 310.
5 D. Dollimore and T. J. Taylor, Thermochim. Acta, 40 (1980) 297.
6 D. Dollimore and T. J. Taylor, Thermal Anal. Proc. 7th ICTA, 1, II (1982) 636.
7 I. M. Uzunov and D. G. Klissurski, Thermochim. Acta, 81 (1984) 353.
8 H. Henmi and T. Hirayama, Thermochim. Acta, 96 (1985) 145.

9 H. Henmi and T. Hirayama, Thermochim. Acta, 106 (1986) 263.
10 R. C. Weast (Ed.), Handbook of Chemistry and Physics (57th ed.) CRC Press, New York 1976.
11 T. Ozawa, J. Thermal Anal., 2 (1970) 301.
12 T. Ozawa, J. Thermal Anal., 9 (1976) 369.
13 K. F. Baker, Du Pont, Instruments, Thermal Analysis Application Brief, No. TA-53.
14 C. Heald and A. C. K. Smith, Applied Physical Chemistry, Macmillan Press Ltd., London 1982, pp. 20–40.
15 S. A. A. Mansour, Thermochim. Acta, 228 (1993) 155.
16 W. Frank *et al.* (Eds.), Powder Diffraction File for Inorganic Phase, Int. Center for Diffraction Data, Philadelphia, PA, 1981.
17 J. A. Goldsmith and S. D. Ross, Spectrochim. Acta, 24A (1968) 2131.
18 M. K. Soguin, Can. Mineral, 13 (1975) 127.
19 F. F. Bently, L. D. Smithson and A. L. Rozek, Infrared Spectra and Characteristic Frequencies ~700–300 cm^{-1} John Wiley and Sons, USA, 1968, p. 1517.

Zusammenfassung — Mittels TG, DTA und DSC wurde bei verschiedenen Aufheizgeschwindigkeiten die thermische Zersetzung von basischem Kupfercarbonat BCuC (Malachit; $CuCO_3 \cdot Cu(OH)_2$) in dynamischer Luft- oder Stickstoffatmosphäre untersucht. Dabei wurden die nichtisothermen kinetischen und thermodynamischen Parameter geschätzt. Mittels IR, XRD und SEM wurde der Zersetzungsweg umfassend durch die Untersuchung der strukturellen und morphologischen Folgen des Kalzinierens des Materiales verfolgt. Die erhaltenen Resultate zeigen, daß $CuCO_3 \cdot Cu(OH)_2$ in Luft bei 195°C $0{,}5H_2O$ abgibt und in die Azuritstruktur $2CuCO_3 \cdot Cu(OH)_2$ umwandelt. Anschließend beginnt die Zersetzung über zwei endotherme Schritte mit Maximum bei 325 und bei 430°C. Die resultierenden Produkte behalten das im Zersetzungsprozeß freigesetzte Wasser bis 650–750°C bei. Mit Hilfe der thermischen und physikoanalytischen Ergebnisse wurde ein Reaktionsschema vorgeschlagen.